Enhancement of the Thermal Stability and Mechanical Hardness of Zr-Al-Co Amorphous Alloys by Ag Addition

YONGYONG WANG, XIAO DONG, XIAOHUI SONG, JINFENG WANG, GONG LI, and RIPING LIU

The thermal and mechanical properties of $Zr_{57}Al_{15}Co_{28-X}Ag_X$ ($X = 0$ and 8) amorphous alloys were investigated using differential scanning calorimetry, *in situ* high-pressure angle dispersive X-ray diffraction measurements with synchrotron radiation, and nanoindentation. Results show that Ag doping improves effective activation energy, nanohardness, elastic modulus, and bulk modulus. Ag addition enhances topological and chemical short-range orderings, which can improve local packing efficiency and restrain long-range atom diffusion. This approach has implications for the design of the microstructure- and property-controllable functional materials for various applications.

DOI: 10.1007/s11661-016-3388-8

I. INTRODUCTION

BULK amorphous alloys have attracted worldwide interest since the syntheses of bulk amorphous alloys in multicomponent *via* the copper mold casting method in 1988.[1] Considerable effort has been expended to develop new bulk amorphous alloys that possess high stability and useful engineering properties.[2–10] Subsequently, bulk amorphous alloy systems have been widely extended to various-based alloys. Among the bulk glassy alloy systems, the Zr-based alloys exhibit high glass form ability (GFA) and high mechanical strength combined with high ductility; hence, these alloys have attracted much interest as a new type of bulk structural materials. Inoue *et al.*[11] developed Zr-Al-Co-based bulk glassy alloy system. This ternary Zr-based glassy alloy has several excellent features that are not present in quaternary and five Zr-based bulk glassy alloys. The element doping method is widely used in discovering new bulk glass-forming alloys and improving alloy properties.[12] Previous studies found that adding appropriate amount of Ag can enhance the GFA and corrosion resistance, as well as the plasticity of the Zr-Al-Co-based bulk glassy alloys.[13,14] However, the mechanism of the effects of Ag addition on the thermal and mechanical properties of Zr-based glass remains unclear.

This paper aims to examine the effects of Ag addition on the thermal and mechanical properties of $Zr_{57}Al_{15}Co_{28}$ amorphous alloys and reveal the mechanism of Ag addition. The samples were produced by melt spinning. Differential scanning calorimetry (DSC), *in situ* high-pressure angle dispersive X-ray diffraction (ADXRD), and nanoindentation were employed for analyses. The diffraction data in reciprocal space and the atomic pair distribution function (PDF) g(r) in real space were also analyzed.

II. EXPERIMENTS

Alloy ingots were prepared by arc melting the mixtures of pure Zr (99.9 pct), Al (99.9 pct), Co (99.999 pct), and Ag (99.99 pct) in a Ti-gettered argon atmosphere. The amorphous alloy was produced by melt spinning to form ribbons with a cross-section of 0.02×1.2 mm^2 in an argon atmosphere. X-ray diffraction (XRD) was conducted with a D/MAX-2500/PC diffractometer using Cu-$K_{\alpha 1}$ radiation ($\lambda = 1.54$ Å) to characterize the sample structure. Microanalysis was carried out using an energy-dispersive system (EDS) attached to a scanning electron microscope. DSC was also performed with NETZSCH STA449C under a high-purity Ar atmosphere to evaluate thermal behavior. ADXRD measurement was conducted at the beamline 4W2 at the Beijing Synchrotron Radiation Facility. The powder sample prepared by grinding the amorphous ribbon with a pressure calibrator ruby powder was loaded into a 200-μm diameter hole of a

YONGYONG WANG, Associate Professor, is with the College of Physics and Electronic Engineering, and Henan Key Laboratory of Photovoltaic Materials, Henan Normal University, Xinxiang 453007, P. R. China, and also with the State Key Laboratory of Metastable Materials Science and Technology, Yanshan University, Qinhuangdao 066004. Contact e-mail: wangyy@htu.edu.cn XIAO DONG, XIAOHUI SONG, and JINFENG WANG, Associate Professors, are with the College of Physics and Electronic Engineering, and Henan Key Laboratory of Photovoltaic Materials, Henan Normal University, Xinxiang 453007. GONG LI, Professor, is with the State Key Laboratory of Metastable Materials Science and Technology, Yanshan University, and also with the Department of Materials Science and Engineering, The University of Tennessee, Knoxville, TN37996. Contact e-mail:gli25@utk.edu RIPING LIU, Professor, is with the State Key Laboratory of Metastable Materials Science and Technology, Yanshan University.

Manuscript submitted September 17, 2015.
Article published online February 18, 2016

T301 stainless steel gasket. More experimental details are found in Reference 15. Nanoindentation testing was carried out using a Hysitron TriboIndenter with a diamond Berkovich tip having a curvature radius of 260 nm. The constant contact force and the amplitude of the sinusoidal force were 2 and 0.25 μN, respectively. More experimental details are found in Reference 16. Atomic PDF g(r) was obtained using the PDFgetX2 program.[17]

III. RESULTS

The ribbon structure was ascertained *via* XRD (Figure 1). The broad diffraction maximum and the absence of Bragg peaks corresponding to crystalline phase indicate that the fully amorphous ribbons were obtained for the amorphous alloys.

Non-isothermal crystallization kinetic behavior was measured through DSC at different heating rates (*i.e.*, 10, 20, 30, and 40 K/min) to investigate the effects of Ag doping on the thermal behavior of $Zr_{57}Al_{15}Co_{28}$ amorphous alloys. Subsequently, the characteristic peak temperatures were derived from the DSC measurements. The activation energy of the present amorphous alloy can be estimated using the Kissinger equation[18]:

$$\ln\left(\frac{T_\theta^2}{\beta}\right) = \frac{E_\theta}{RT_\theta} + \text{const}, \qquad [1]$$

where β is the heating rate; T_θ represents the characteristic temperatures, such as T_g, T_x, and T_p (crystallization peak temperature); and R denotes the gas constant. The related effective activation energies were obtained by plotting $\ln(T^2/\beta)$ *vs* $1/T$ for the samples (Figure 2) and are summarized in Table I. The onset crystallization temperature of an amorphous alloy generally refers to the start of crystal precipitation from the amorphous matrix, and the peak temperature corresponds to the start of crystal collision.

Therefore, the onset crystallization temperature is speculated to be strongly associated with nucleation, and the peak temperature is related with growth.[19] Moreover, presuming that the activation energy calculated from the onset temperature represents the activation energy for nucleation E_n, which corresponds to the short-range diffusion and rearrangement barrier of atoms, and that the other value denotes the activation energy for growth E_g, which represents the long-range diffusion, seems reasonable. Ag doping improves the effective activation energies E_n and E_g. This result indicates that Ag doping could hinder the diffusion of atoms and enhance the thermal stability of $Zr_{57}Al_{15}Co_{28}$ amorphous alloys to a certain extent.

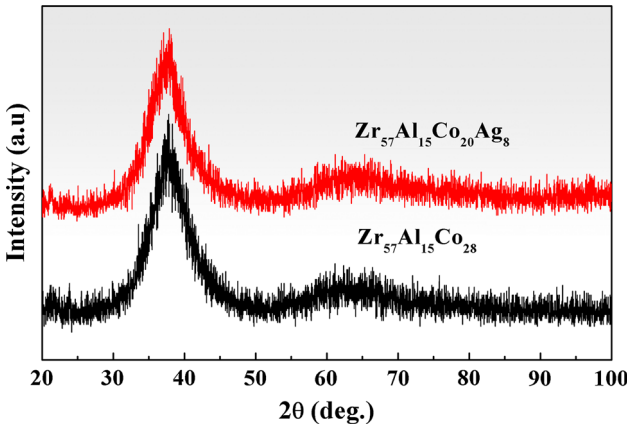

Fig. 1—X-ray diffraction patterns of $Zr_{57}Al_{15}Co_{20}Ag_8$ and $Zr_{57}Al_{15}Co_{28}$ amorphous alloys.

Nanoindentation was employed to determine the mechanical properties of the alloys. The hardness and elastic modulus were calculated using the load-displacement and unloading curves according to the procedure suggested by Oliver and Pharr.[20] Table II summarizes the mechanical properties, such as nanohardness, elastic modulus, and ratio of nanohardness and elastic modulus (H/E) of the alloys. The nanohardness and elastic modulus clearly increase with Ag addition. The H/E ratios are 0.079 and 0.073 for the $Zr_{57}Al_{15}Co_{28-X}Ag_X$ (X = 0 and 8) alloys, respectively. The increase in mechanical properties results from structure evolution *via* Ag addition.

The stability of $Zr_{57}Al_{15}Co_{28-X}Ag_X$ (X = 0 and 8) amorphous alloys under high pressure was investigated using ADXRD. Figure 3 shows the synchrotron radiation XRD at different pressures for $Zr_{57}Al_{15}Co_{28-X}Ag_X$ (X = 0 and 8) amorphous alloys. The broad halo remained unaltered until 47.8 GPa, thereby indicating the fully amorphous structure of sample during the measurements. The diffusive amorphous hole evidently shifted to larger 2-theta values because of the compression effect.

Obtaining the equation of state is necessary to gain a better understanding of the effect of Ag addition on the structure of $Zr_{57}Al_{15}Co_{28}$ amorphous alloys. Bridgman presented the EOS as follows[21]:

$$-\Delta V/V_0 = a_0 + aP + bP^2 + cP^3 + \cdots, \qquad [2]$$

where V_0 is the volume at zero pressure and coefficients a_0, a, b, and c can be determined *via* the least squares method. The relative volume change ($\Delta V/V_0$ ($\Delta V = V_P - V_0$)) at a given pressure (V_P) to that at zero pressure (V_0) can be estimated. The experimental $\Delta V/V_0 \sim P$ data can be obtained from the synchrotron radiation XRD spectrum, and the results are shown in Figure 4. Bulk modulus B can be obtained according to the relationship $B = 1/a$. Bulk modulus B for the $Zr_{57}Al_{15}Co_{28}$ and $Zr_{57}Al_{15}Co_{20}Ag_8$ alloys are 130.03 and 138.31 GPa, respectively. High bulk modulus indicates a relatively hard material. The result indicates that Ag addition can improve the mechanical property of $Zr_{57}Al_{15}Co_{28}$, which is consistent with our nanoindentation experiment.

IV. DISCUSSIONS

The short-to-medium range order in amorphous materials is manifested by the peak of atomic PDF g(r) at small r. The structure information is embedded in

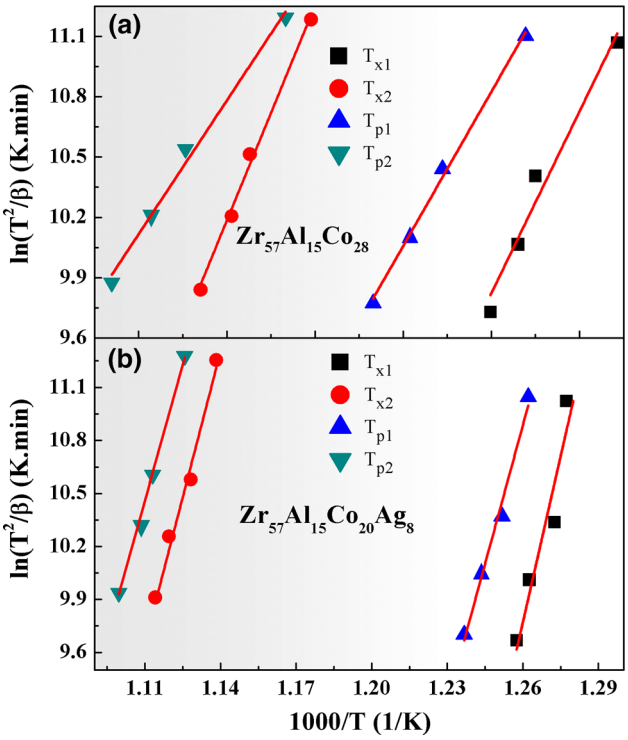

Fig. 2—Kissinger's plot of T_p and T_x for $Zr_{57}Al_{15}Co_{28}$ (*a*) and $Zr_{57}Al_{15}Co_{20}Ag_8$ (*b*) amorphous alloys.

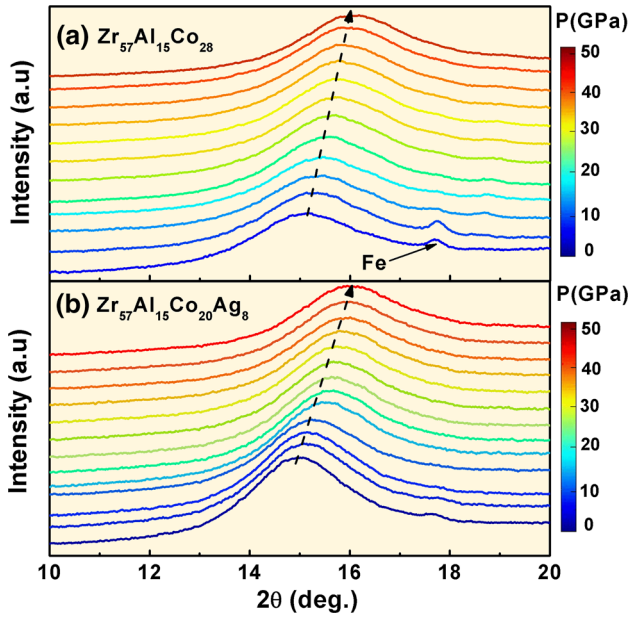

Fig. 3—Angle-dispersion X-ray diffraction patterns of $Zr_{57}Al_{15}Co_{28}$ (*a*) and $Zr_{57}Al_{15}Co_{20}Ag_8$ (*b*) amorphous alloys.

the peak position, width, and relative intensity. To elucidate the structural evolution of the specimens with Ag addition more accurately, the atomic PDF g(*r*) was obtained by the PDFgetX2 program.[17] Figure 5 displays the atomic PDF g(*r*) for the $Zr_{57}Al_{15}Co_{28}$ and $Zr_{57}Al_{15}Co_{20}Ag_8$ alloys at ambient pressure. The differences in the two curves indicate the presence of structural changes with Ag addition. Differences occur in the peak position and intensity pointing to changes of the atomic arrangements with Ag addition, where the topological short-to-medium range order was changed. The peak positions are shifted to lower values, indicating that the averaged atomic distance is decreased with Ag addition. In the Zr-Al-Co-Ag system, the atomic radii of Zr, Al, Co, and Ag are 0.160, 0.143, 0.126, and 0.145 nm, respectively. The Ag size is between that of Zr and Al, and Ag addition causes a more sequential change in atomic size, such that Zr >> Ag > Al >> Co. Hence, Ag doping can produce an efficiently dense random packing structure, which increases the packing density in the amorphous alloys. High packing density results in high thermal stability and nanohardness of amorphous alloys.

The packing structure of amorphous alloys can be generally described by a dense cluster model.[22–24] This model demonstrates that the SROs of amorphous alloys are characterized by solute-centered clusters, each of which is made up of a solute atom surrounded by a majority of solvent atoms. Adjacent clusters share solvent atoms in common faces, edges, or vertices so that neighboring clusters overlap in the first coordination shell. The precise form of these polyhedral clusters is controlled by the ratio of the effective sizes of solute and solvent atoms, and the form changes according to

Table I. Crystallization Activation Energy of $Zr_{57}Al_{15}Co_{28}$ and $Zr_{57}Al_{15}Co_{20}Ag_8$ Amorphous Alloys

Alloys	E_{x1} (kJ/mol)	E_{x2} (kJ/mol)	E_{p1} (kJ/mol)	E_{p2} (kJ/mol)
$Zr_{57}Al_{15}Co_{28}$	375.928	444.274	318.739	276.033
$Zr_{57}Al_{15}Co_{20}Ag_8$	521.529	456.923	434.831	426.176

Table II. Nanohardness *H* (GPa), Elastic Modulus *E* (GPa), and *H*/*E* Ratio of the Alloys

Alloys	*H* (GPa)	*E* (GPa)	*H*/*E*
$Zr_{57}Al_{15}Co_{28}$	7.438	93.578	0.079
$Zr_{57}Al_{15}Co_{20}Ag_8$	8.465	115.697	0.073

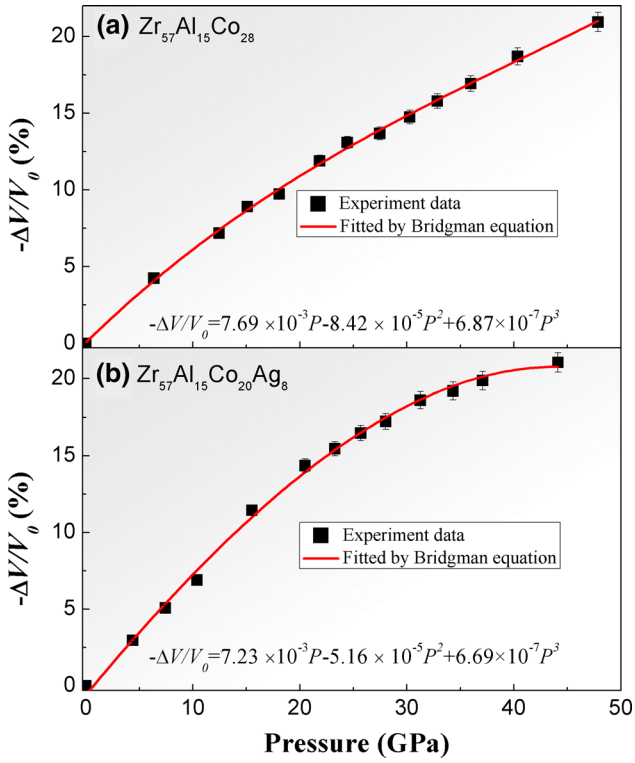

Fig. 4—Pressure dependence of relative volume change $\Delta V/V_0$ of $Zr_{57}Al_{15}Co_{28}$ (*a*) and $Zr_{57}Al_{15}Co_{20}Ag_8$ (*b*) alloys at ambient temperature.

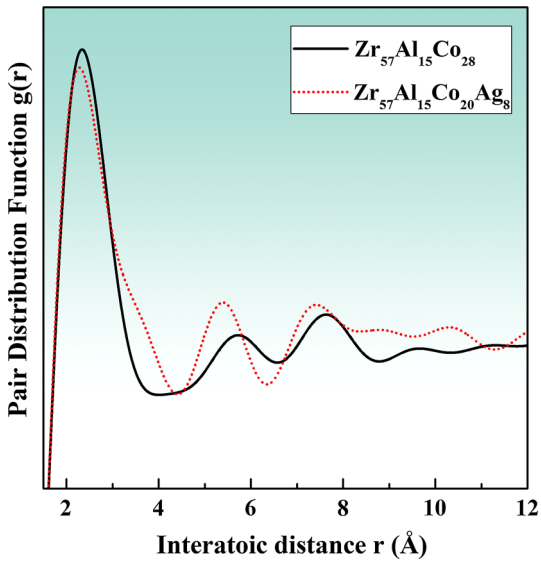

Fig. 5—Comparison of the atomic pair distribution function (PDF) g(*r*) of $Zr_{57}Al_{15}Co_{28}$ and $Zr_{57}Al_{15}Co_{20}Ag_8$ alloys.

the elemental constituents of the glass. Therefore, the improved activation energy, hardness, and elastic modulus of the amorphous alloys are presumed to originate from the increasing packing fraction in the amorphous structure *via* Ag addition. This concept was confirmed by the previous[25] and present results.

V. CONCLUSIONS

The effects of Ag doping on the thermal and mechanical properties of $Zr_{57}Al_{15}Co_{28}$ alloys were investigated. Ag addition changed the chemical and topological short-range ordering of alloys, thereby resulting in an increased local packing efficiency of $Zr_{57}Al_{15}Co_{28}$ alloys. The amorphous structure with dense atomic configuration and strong bonding force may increase the difficulty of the diffusivity of constituent atoms, hence leading to an increase in the activation energy and mechanical properties of the alloys. The nanohardness increases from ~7.4 to ~8.4 GPa, and the elastic modulus increases from ~93.5 to ~115.6 GPa.

ACKNOWLEDGMENTS

This work was supported by the National Natural Science Foundation of China (Grant No. 51271161/51171163/51121061), PhD research startup foundation of Henan Normal University (Grant No. qd208), Foundation of Henan Educational Committee (Grant No. 15A140007/15A140008), and Henan Province Foundation and Advanced Technology Research Program (Grant No. 122300410230). Gong Li would like to acknowledge the Specialized Research Fund for the Doctoral Program of Higher Education (Grant No. 20131333110019).

REFERENCES

1. A. Inoue, K. Ohtera, K. Kita, and T. Masumoto: *Jpn. J. Appl. Phys.*, 1988, vol. 27, pp. L2248–51.
2. C.R. Cao, Y.M. Lu, H.Y. Bai, and W.H. Wang: *Appl. Phys. Lett.*, 2015, vol. 107, p. 141606.
3. X.F. Zhang, Y.M. Wang, J.B. Qiang, Q. Wang, D.H. Wang, D.J. Li, C.H. Shek, and C. Dong: *Intermetallics*, 2004, vol. 12, pp. 1275–1278.
4. Z. Wang, J.W. Qiao, H. Tian, B.A. Sun, B.C. Wang, B.S. Xu, and M.W. Chen: *Appl. Phys. Lett.*, 2015, vol. 107, p. 201902.
5. K.J. Laws, D.B. Miracle, and M. Ferry: *Nat Commun.*, 2015, vol. 6, p. 8213.
6. T. Wada, F.X. Qin, X.M. Wang, M. Yoshimura, and A. Inoue: *J. Mater. Res.*, 2009, vol. 24, pp. 2941–48.
7. S.V. Ketov, Y.H. Sun, S. Nachum, Z. Lu, A. Checchi, A.R. Beraldin, H.Y. Bai, W.H. Wang, D.V. Louzguine-Luzgin, M.A. Carpenter, and A.L. Greer: *Nature*, 2015, vol. 524, pp. 200–203.
8. H.T. Zong, M.Z. Ma, X.Y. Zhang, L. Qi, G. Li, Q. Jing, and R.P. Liu: *Chin. Phys. Lett.*, 2011, vol. 28, p. 036103.
9. Y.C. Hu, F.X. Li, M.Z. Li, H.Y. Bai, and W.H. Wang: *Nat. Commun.*, 2015, vol. 6, p. 8310.
10. H.T. Zong, M.Z. Ma, L.M. Wang, and R.P. Liu: *J. Appl. Phys.*, 2010, vol. 107, p. 053515-1/-4.
11. T. Zhang and A. Inoue: *Mater. Trans.*, 2002, vol. 43, pp. 1250–53.
12. S.V. Madge and A.L. Greer: *Mater. Sci. Eng. A.*, 2004, vol. 375, p. 759.
13. C. Zhang, N. Li, J. Pan, S.F. Guo, M. Zhang, and L. Liu: *J. Alloys Compd.*, 2010, vol. 504S, pp. S163–67.
14. Z. Liu, K.C. Chan, and L. Liu: *J. Alloys Compd.*, 2009, vol. 487, pp. 152–156.
15. G. Li, Y.C. Li, Z.K. Jiang, T. Xu, L. Huang, J. Liu, T. Zhang, and R.P. Liu: *J. Non-Cryst. Solids*, 2009, vol. 355, pp. 521–24.
16. Y.Y. Wang, W. Zhao, G. Li, and R.P. Liu: *J. Alloys Comp*, 2012, vol. 544, pp. 46–49.
17. P.F. Peterson, M. Gutmann, T. Proffen, and S.J.L. Billinge: *J. Appl. Cryst.*, 2000, vol. 33, p. 1192–1192.
18. H.E. Kissinger: *Anal. Chem.*, 1957, vol. 29, pp. 1702–06.

19. H.R. Wang, Y.L. Gao, G.H. Min, X.D. Hui, and Y.F. Ye: *Phys. Lett. A*., 2003, vol. 314, pp. 81–87.
20. W.C. Oliver and G.M. Pharr: *J. Mater. Res*., 1992, vol. 7, pp. 1564–83.
21. P.W. Bridgman: *The Physics of High Pressure*, G. Bell and Sons Ltd., London, 1958.
22. D.B. Miracle: *Nat. Mater*., 2004, vol. 3, pp. 697–702.
23. D. Ma, A.D. Stoica, X.-L. Wang, Z.P. Liu, B. Clausen, and D.W. Brown: *Phys. Rev. L*., 2012, vol. 108, p. 085501.
24. A.R. Yavari: *Nature*., 2006, vol. 439, pp. 405–06.
25. N.B. Hua, S.J. Pang, Y. Li, J.F. Wang, R. Li, K. Georgarakis, A.R. Yavari, G. Vaughan, and T. Zhang: *J. Mater. Res*., 2011, vol. 26, pp. 539–46.